

EFFECTS OF ALUMINUM AND COPPER ON THE GRAPHITE MORPHOLOGY, MICROSTRUCTURE, AND COMPRESSIVE PROPERTIES OF DUCTILE IRON

H. Sazegaran ^{a,*}, F. Teimoori ^a, H. Rastegarian ^a, A.M. Naserian-Nik ^b

^aQuchan University of Technology, Department of Industrial Engineering, Faculty of Engineering, Quchan, Iran

^bQuchan University of Technology, Department of Mechanical Engineering, Faculty of Engineering, Quchan, Iran

(Received 24 December 2019; Accepted 11 January 2021)

Abstract

The effect of aluminum (0, 2, 4, and 6 wt. %) and copper (0, 2, 4, and 6 wt. %) on graphite morphology, microstructure and compressive behavior of ductile iron specimens manufactured by sand casting technique were investigated. The graphite morphology and microstructure were evaluated using optical microscopy (OM) and scanning electron microscopy (SEM) equipped image processing software. To study the mechanical properties, the compression test was conducted on the ductile iron specimens. The results indicated that the surface fraction and nodule count of graphite decreased when the amount of aluminum increased from 0 to 2 wt. % and after that from 2 to 6 wt. %. In addition, the nodularity of graphite increased with the increment of the aluminum amounts. By adding the amount of copper, the surface fraction and nodule count of graphite increased and nodularity of graphite decreased. The addition of aluminum and copper decreased the surface fraction of ferrite and increased the surface fraction of pearlite in the microstructure. By increasing the amounts of aluminum and copper, compressive stress vs. strain curves were shifted upwards, and modulus of elasticity, yield strength, maximum compressive stress, and fracture strain improved. In comparison with copper, aluminum had a greater influence on the mechanical properties of ductile iron.

Keywords: Ductile iron; Copper; Aluminum; Graphite morphology; Microstructure; Compressive properties

1. Introduction

Cast iron is a group of advantageous engineering alloys that can be applied in many structural and non-structural applications due to its attractive combination of properties such as low cost, high density, low melting point, good castability and machinability, excellent wear and corrosion resistance, high stiffness and compressive strength, exclusive thermal conductivity, and good vibration damping characteristics [1-3]. The industrial applications of cast irons can be increased by improving the mechanical properties [4, 5]. The modification of the chemical composition, controlling the cooling and solidification rates during the casting processes, and the proper heat treatment, can improve the graphite morphology and the microstructure of cast irons, resulting in improved mechanical properties [6-9].

It is known that the heat treatment, especially austempering in gray and ductile cast irons, leads to an increase in the final cost [11, 12]. Also, it is difficult to control the cooling and solidification rates

in the sand mold casting techniques [13]. Thus, the modification of the chemical composition by adding the appropriate alloying elements is the best method to improve the mechanical properties and performance of cast irons [14]. Among the various categories of cast irons, the ductile irons have enhanced mechanical behavior due to the formation of nodular graphite [10]. It is shown that the alloying elements have various effects on graphite morphology, microstructure, and mechanical properties of ductile irons. Silicon is often regarded as a highly graphitizing element which prevents the chilling tendency and the precipitation of carbides in the microstructure [15]. Nickel, manganese, and copper are often recognized as austenite stabilizing elements and, due to high electrochemical potential, enhance the corrosion resistance of cast irons, especially austenitic cast irons [16]. In addition, proper heat treatment in cast irons containing nickel, manganese, and copper can improve the wear and corrosion resistance [17, 18].

Adding copper to the cast irons improves the

Corresponding author: h.sazegaran@qiet.ac.ir

<https://doi.org/10.2298/JMMB191224006S>



hardness and the strength [19]. Also, copper reduces the friction coefficient and, as a result, increases the wear resistance. The addition of large amounts of copper causes forming of the white cast iron and, consequently, the alloy becomes brittle and the toughness decreases [20]. It was reported that copper increases the rate of homogenous nucleation and the niobium leads to growth and, therefore, the crystalline structure is formed [21]. In cast iron-based bulk amorphous alloy, the minor Al addition enhances not only the glass-forming ability, but also the nanocrystallization behavior [22]. Adding aluminum to the cast irons reduces the amount of graphite and as well as the wear resistance at elevated temperatures [23]. Chromium improves the wear resistance by increasing the volume fraction of chromium carbide [24]. Adding low amounts of molybdenum results in the higher thermal conductivity and high amounts of molybdenum increase the precipitation and solid solution strengthening, thus improving the strength [25]. Although many studies are focused on the influences of the affecting factors on the microstructure, mechanical properties, and performance of the cast irons, the effect of 0, 2, 4, and 6 wt. % of aluminum and copper is not investigated in ductile iron. The objective of this work is to study the effects of aluminum and copper additives on the graphite morphology, microstructure, and compressional properties of ductile iron.

2. Materials and experimental method

2.1. Materials and casting technique

In this study, ductile iron specimens containing different amounts of aluminum and copper were manufactured by sand mold casting method. Silica sand with 5 wt. % sodium silicate, as binder, was used in the molding process. The prepared molds contained cylindrical cavities with a diameter of 20 mm and height of 200 mm. After molding, the mold surfaces were exposed to carbon dioxide gas and after the reaction of sodium silicate with carbon dioxide, the strength of the molds was enhanced. The schematic pattern and mold are shown in Fig.1. The raw materials used in this work were: mild steel scrap (0.25 wt. % C, 0.3 wt. % Si, and 0.5 wt. % Mn), ductile iron returns (3.43 wt. % C and 1.87 wt. % Si), carbon (90 wt. % C), ferro-silicon (0.5 wt. % C and 75 wt. % Si), pure copper (99.9 wt. % Cu), and pure aluminum (99.9 wt. % Al). The molten iron was prepared using an industrial medium-frequency coreless induction furnace with a capacity of 1 ton (at Kaveh Steel Foundry). The power consumption of the furnace was 550 kW. In the melting process, carbon and silicon were added into the molten iron up to the appropriate amounts. The chemical composition of the molten iron is presented in Table 1.

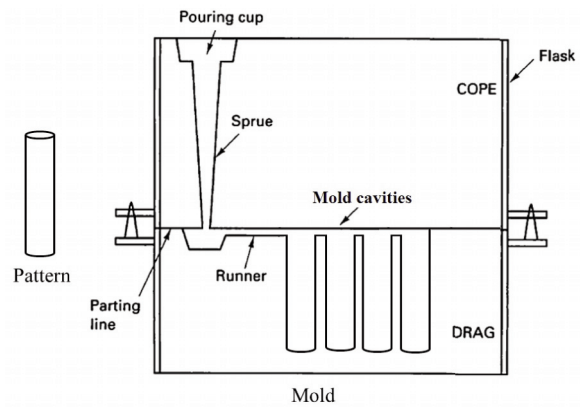


Figure 1. Schematic pattern and mold to manufacture different specimens

Table 1. Chemical composition of the ductile iron specimens, wt. %

CE	C	Si	Al	Ni	Mn	P	S	Mg	Fe
4.24	3.67	2.06	0.02	0.03	0.07	<0.005	<0.005	0.06	Bal.

The sandwich technique was applied to add magnesium to the molten iron and spheroidizing process with Fe-Mg master alloy (containing 8 wt. % Mg) was successfully performed. In this technique, the spheroidizing alloys are covered preferably with the steel sheet. Such a cover delays the reaction. Before pouring process, the molten iron was transferred into a graphite crucible and Fe-Si alloy (65 wt. % Si) was added to the molten iron for inoculation process. The inoculant was there to provide the melt with seeds or nucleation on to which the solid phases grew during freezing as nodules. After removing the slag, the proper amounts of additional aluminum and copper were added into the crucible at different stages and the pouring process was performed at 1390 °C after spheroidizing and inoculation. Then, the cooling and solidification of castings were carried out in the sand molds. As a result, ductile iron specimens containing different amounts of aluminum and copper were manufactured after the break of the mold.

2.2. Graphite morphology and microstructure evaluations

Firstly, casting specimens were cut, hot-mounted, ground, and polished in accordance with standard metallographic procedures (ASTM E2567-11). To study the microstructure of ductile iron specimens, 2% Nital solution was used as proper etchant. The evaluations of optical microscopy were performed on the specimens (before and after etching) and metallographic

images were prepared in various magnifications. The MIP™ image processing software was used to analyze the polished and etched microscopic images. In the optical images of polished surfaces, the morphology of graphite including the surface fraction of graphite, graphite nodule count, and nodularity of graphite were determined. In the optical images of etched surfaces, the microstructural parameters including surface fractions of ferrite and pearlite were measured. To determine the microscopic parameter using the image processing software, 10 images were used for each measurement.

2.3. Mechanical behavior

To determine the mechanical properties, compression tests were conducted on the ductile iron specimens containing various amounts of aluminum and copper. The compression tests were performed according to ASTM E9 standard using Zwick Z250 machine with a cross speed of 1 mm/min. To prepare the compressional specimens, the casting specimens were turned on a metalworking lathe using high speed steel cutting tool. The height and diameter of the

compressional specimens were selected to be 15 and 10 mm, respectively. For each experimental condition, three ductile iron specimens were pressed, at least.

3. Results and Discussion

3.1. Graphite morphology

The graphite morphology (shape, size, surface fraction, distribution, and nodularity), which depended strongly on the chemical composition, had a significant influence on the mechanical properties of ductile cast irons [26]. It is known that spheroidizing the melted iron with reactive elements such as magnesium, calcium, cerium, and other rare earth elements leads to nucleation and growth of spherical graphite and, as a result, ductility and toughness of cast iron increase. As a spheroidizing agent, magnesium has more significant effect on the nodularity of graphite than other elements [27]. The optical microscopy images of as-polished ductile iron specimens containing different amounts of aluminum are shown in Fig. 2. The spheroidizing with magnesium successfully formed the nodular graphite with a relatively uniform distribution. It was

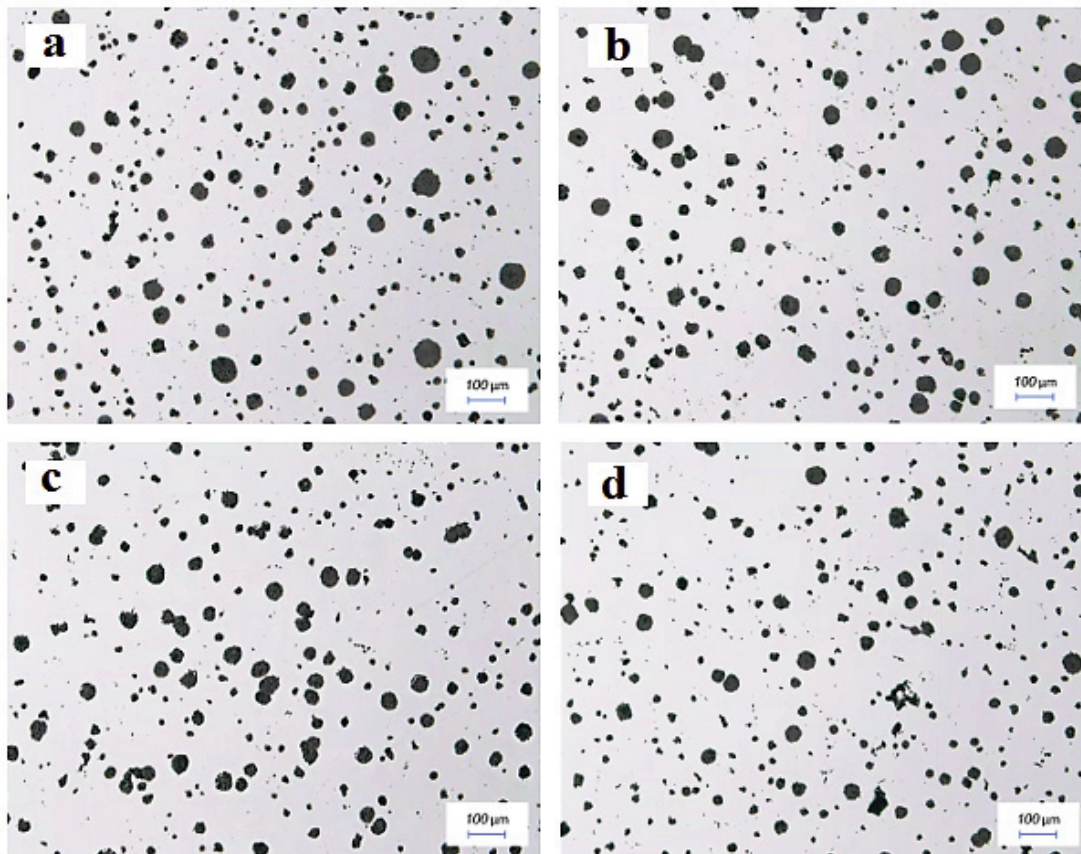


Figure 2. Optical microscopy images of as-polished specimens containing a) 0 wt. % Al, b) 2 wt. % Al, c) 4 wt. % Al, and d) 6 wt. % Al (at 100X magnification)

found that the surface fraction of graphite, number of graphite nodules, and graphite nodularity depended on the addition of aluminum to ductile iron.

The microscopic image processing results of the ductile iron specimens containing different amounts of aluminum are shown in Fig. 3. The results include surface fraction, nodule count, and nodularity of graphite. It was found that the amount of aluminum significantly affected the graphite morphology. By increasing the amount of aluminum up to 2 wt. %, the surface fraction of graphite (Fig. 3-a) and the nodule count of graphite (Fig. 3-b) decreased, and then, increased. Also, graphite nodularity increased by increasing the amount of aluminum. In ductile iron containing low amounts of aluminum, the formation of graphite was restricted and it reduced the surface fraction of graphite [23]. In the ductile iron containing high amounts of aluminum, aluminum is known as a graphitizing element. The effects of aluminum on graphite nucleation and growth is the same as silicon's [28]. In addition, aluminum can positively affect the formation of complex silicates, which these particles are known as nucleation sites of

nodular graphite [27].

In the ductile iron, the copper amounts affected the morphology of graphite [29]. The optical microscopic images of as-polished ductile iron specimens containing various copper amounts are shown in Fig. 4. It can be seen that adding copper to the ductile iron caused the formation of compacted graphite with nodular graphite. The observed compacted graphite was a short flake-like graphite particle with a vermicular or worm-like shape. The results of image processing, including the surface fraction of graphite nodules, nodule count of graphite, and graphite nodularity obtained for the ductile iron specimens containing various copper amounts are shown in Fig. 5. The surface fraction of graphite increased with increasing copper content. Adding copper to ductile iron decreased the graphite nodularity significantly. It was reported that in a ductile iron containing high amounts of copper (up to 1.5 wt. %), the copper islands were formed, and thin layers of copper were observed around the graphite nodules [30]. Also, the Mg_2Cu precipitates were detected in the ductile iron alloyed with copper [31].

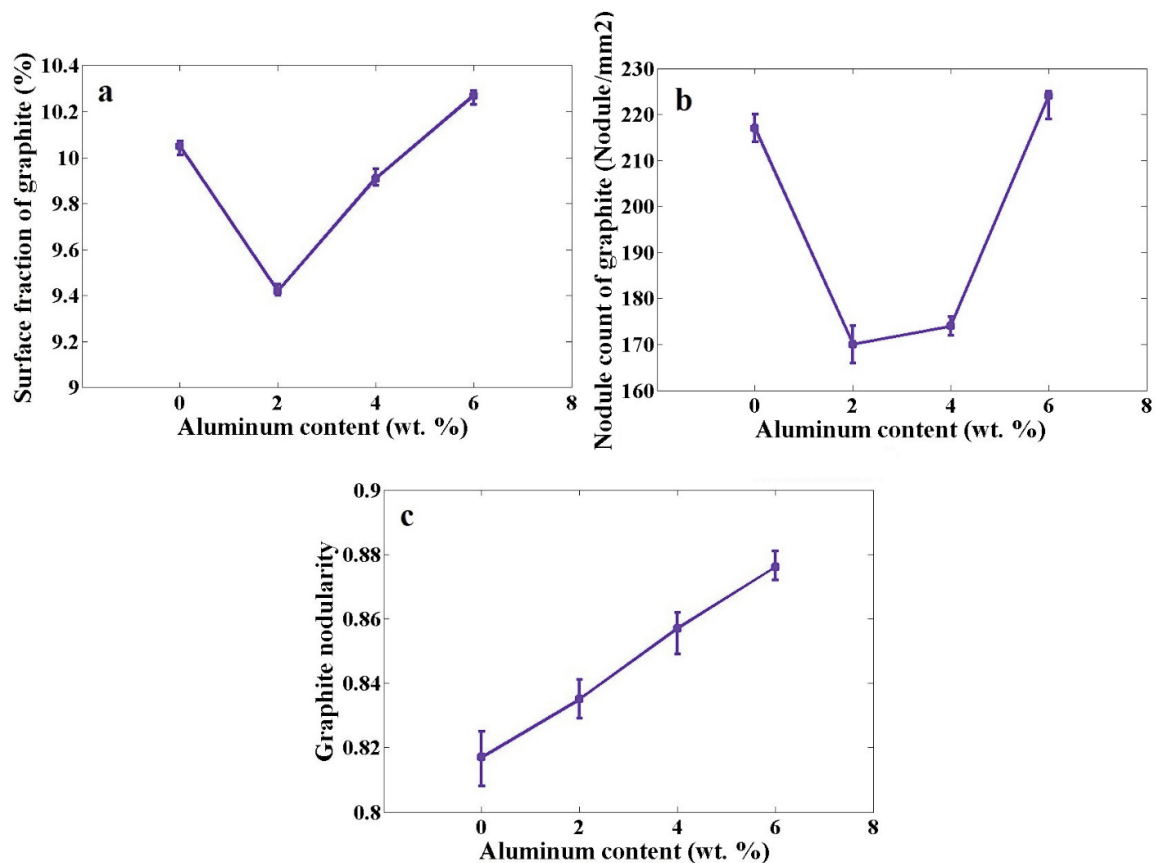


Figure 3. Effect of aluminum content on a) surface fraction of graphite nodules, b) nodule count of graphite, and c) graphite nodularity

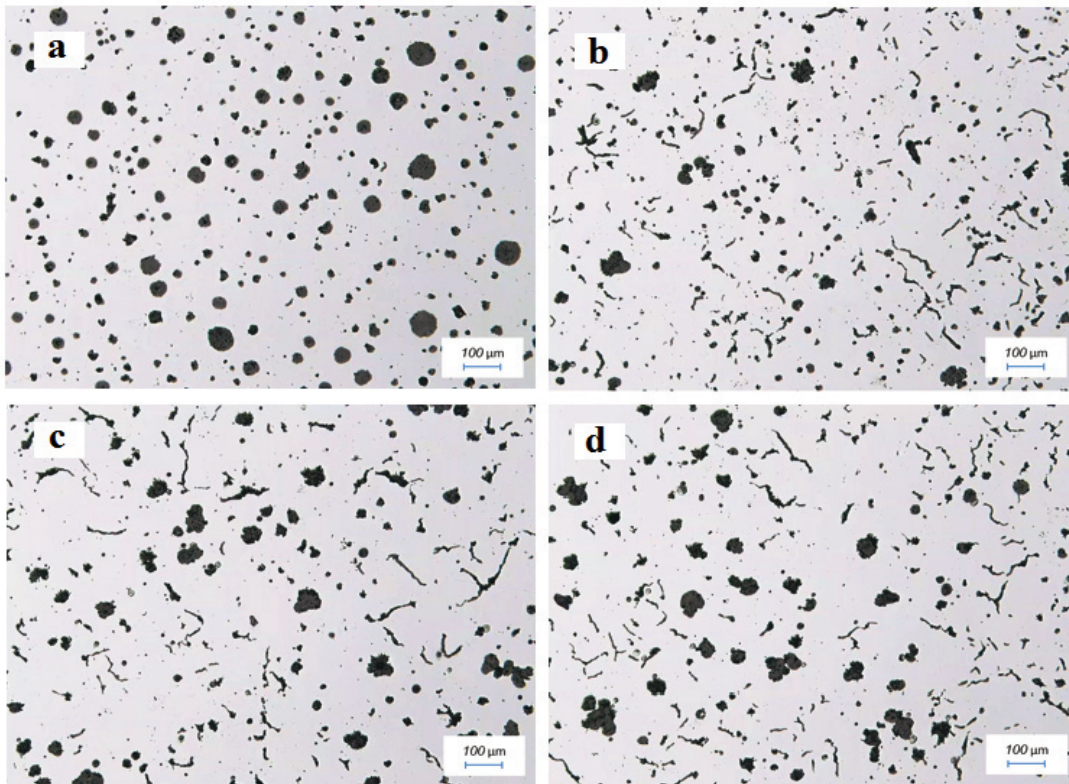


Figure 4. Optical microscope images of as-polished ductile iron specimens containing a) 0 wt. % Cu, b) 2 wt. % Cu, c) 4 wt. % Cu, and d) 6 wt. % Cu

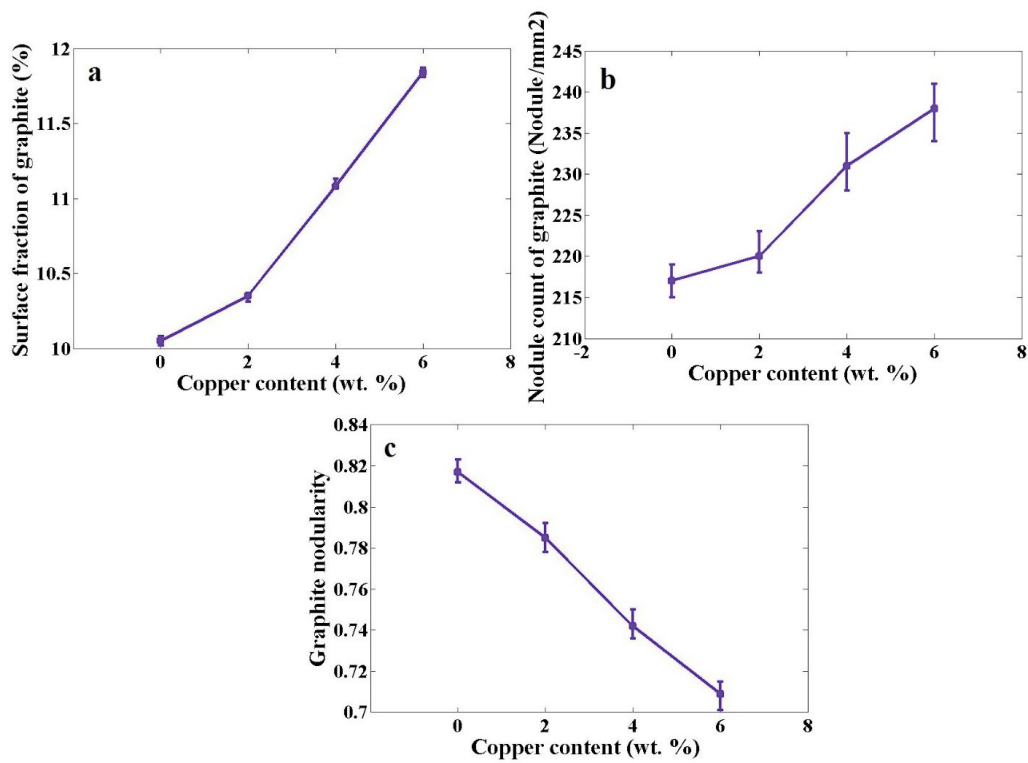


Figure 5. Effect of copper content on a) surface fraction of graphite nodules, b) nodule count of graphite, and c) graphite nodularity



3.2. Microstructural evaluations

The microstructural images of ductile iron specimens with different amounts of aluminum are shown in Fig. 6. It was observed that the microstructure of ductile iron contained the spherical graphite nodules distributed in the ferrite and pearlite. The graphite nodules were encircled by a thin layer of ferrite, known as ferrite halo around graphite nodules. This phenomenon happened because the regions around the growing nodules were decarburized as carbon diffused and deposited on to the graphite nodules. Adding aluminum (from 0.48 to 2.11 wt. %) to the ductile iron decreased the size of spherical graphite nodules, nodule count increment and pearlite to ferrite ratio. It formed a relatively uniform distribution of graphite nodules in the microstructure. Also, the addition of aluminum affected the eutectic temperatures and undercooling degree [32].

The variations of the surface fraction of ferrite and

pearlite for the specimens with aluminum additive obtained from microstructural image processing are depicted in Fig. 7. It demonstrated that a higher amount of aluminum in the ductile iron caused a lower surface fraction of ferrite and higher surface fraction of pearlite. Aluminum affected the rate and the time of carbon diffusion. By increasing the amount of aluminum, the rate of carbon diffusion increased, and thus, more pearlite formed. In addition, an increase in the amount of aluminum caused the formation of aluminum oxide in the molten iron and, as a result, improved the rate of heterogeneous nucleation. It led to an increase in the pearlite to ferrite ratio [33].

The microstructural images of ductile iron specimens containing different amounts of copper are shown in Fig. 8. The images indicated that the microstructure consisted of nodular graphite and compacted graphite distributed in the ferrite and pearlite. A thin layer of ferrite formed around the

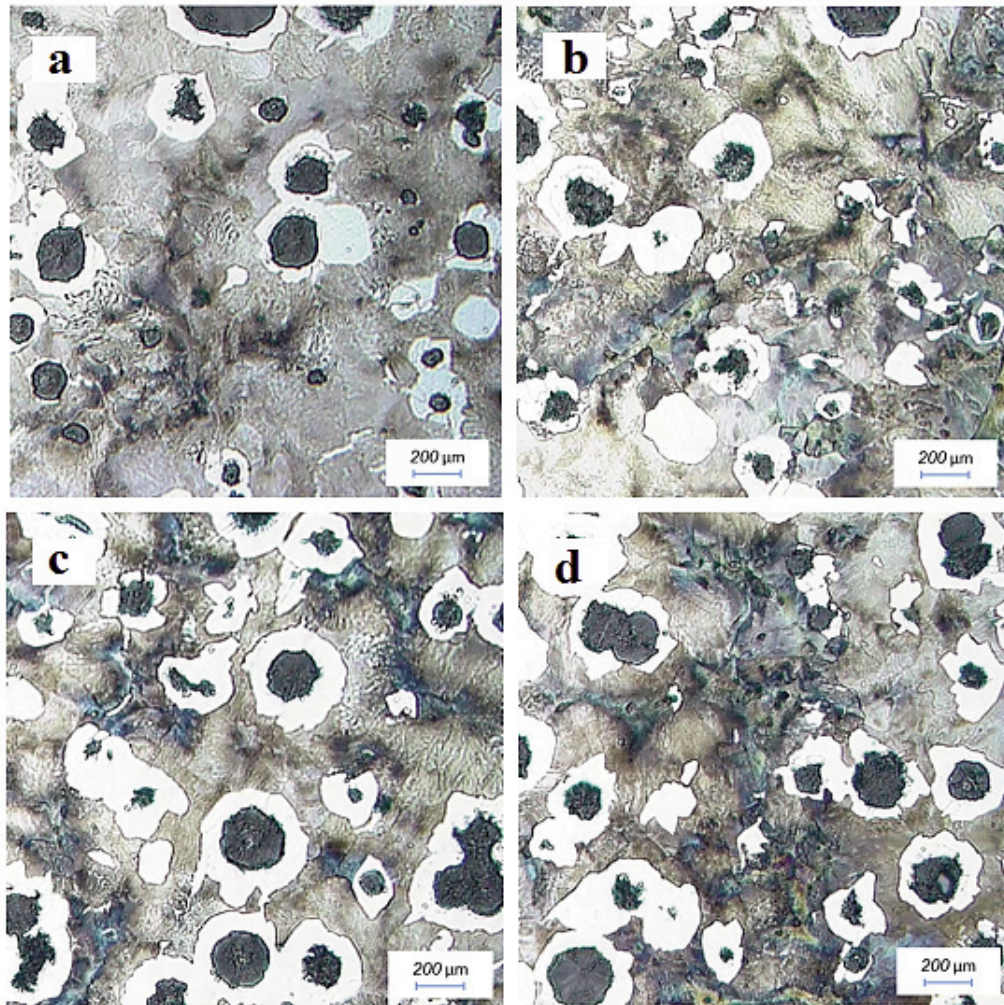


Figure 6. Microstructural images of ductile iron specimens containing a) 0 wt. % Al, b) 2 wt. % Al, c) 4 wt. % Al, and d) 6 wt. % Al (magnification 200X, Nital 2%)

graphite particles, and most of the graphite particles were completely surrounded by the ferrite. The addition of copper caused a significant change in the ductile iron microstructure and resulted in an increase in the pearlite to ferrite ratio [34, 35]. This can be related to eutectoid reactions. Fig. 9 shows the variations of the surface fraction of ferrite and pearlite in the ductile iron specimens with different copper amounts. Adding copper from 0 to 6 wt. % to ductile iron decreased the surface fraction of ferrite and increased the surface fraction of pearlite. By adding copper to ductile iron, carbon diffusion increased in austenite, and as a result, more pearlite can be formed compared to ferrite [31]. It has already

been reported that the amount of pearlite increased sharply with increasing the copper content to 1 wt. % [36]. The SEM images and EDS results of ductile iron specimens without aluminum and copper, containing 4 wt. % of aluminum, and containing 4 wt. % of copper are shown in Fig. 10. In all microstructures, ferrite, pearlite and graphite nodules were clearly observed. Also, iron and carbon peaks formed in the EDS results. Although in the ductile iron containing 1.5 wt. % of copper [30], the formation of copper islands in the microstructure has been previously reported, but in these results no phases containing aluminum and copper were observed.

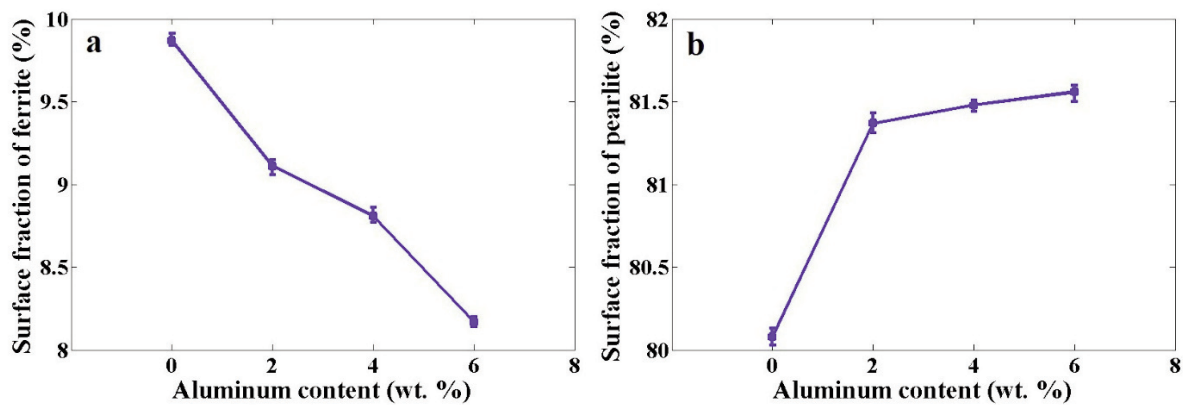


Figure 7. Effect of aluminum content on a) surface fraction of ferrite and b) surface fraction of pearlite

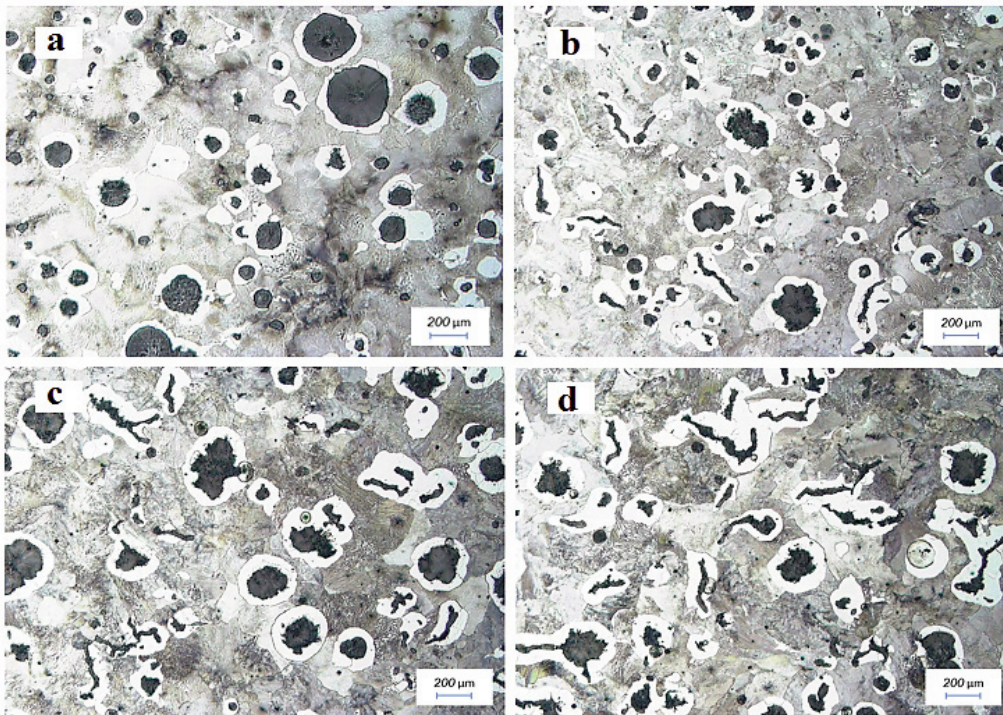


Figure 8. Microstructural images of ductile iron specimens containing a) 0 wt. % Cu, b) 2 wt. % Cu, c) 4 wt. % Cu, and d) 6 wt. % Cu (magnification 200X, Nital 2%)

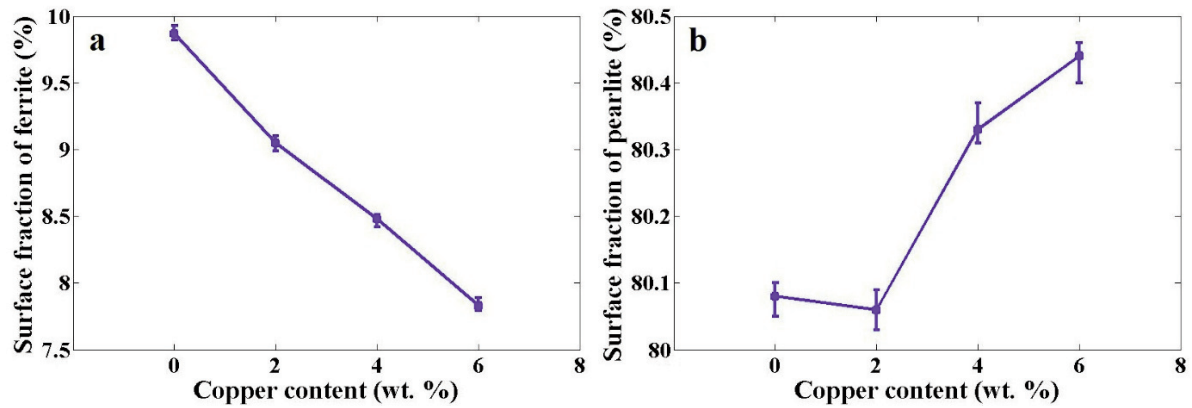


Figure 9. Effect of copper content on a) surface fraction of ferrite and b) surface fraction of pearlite

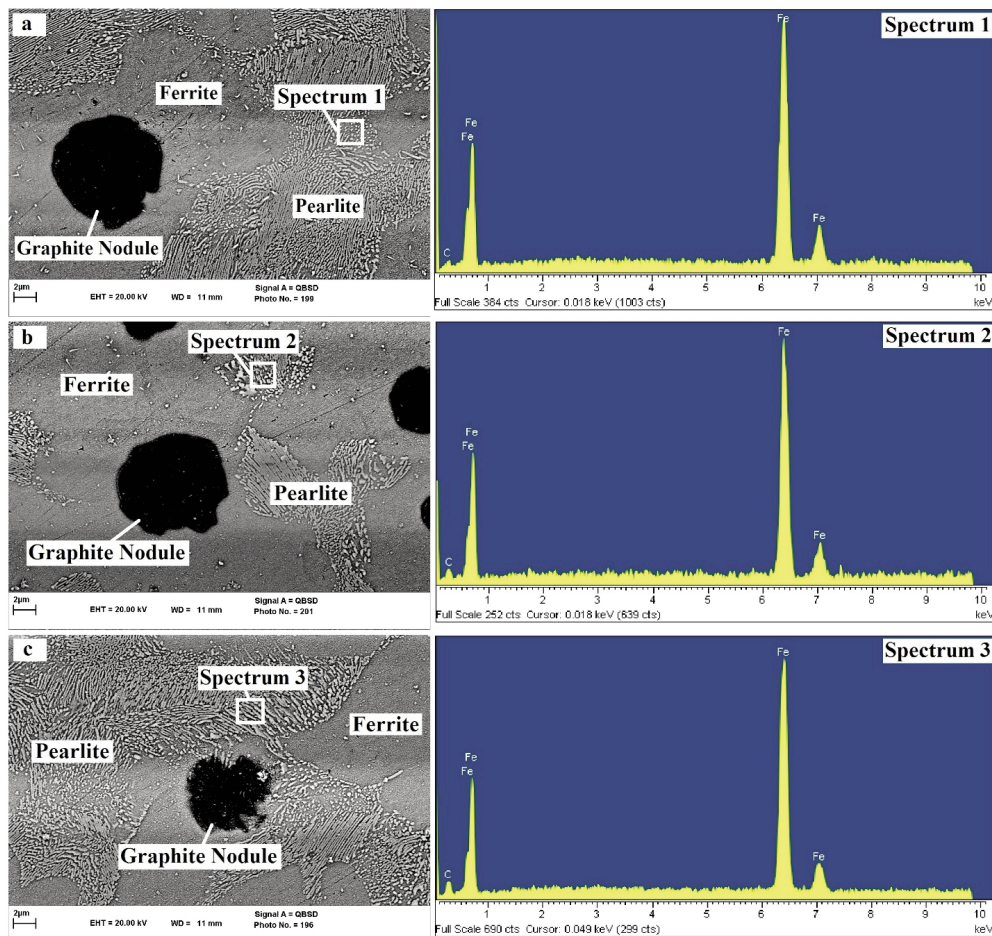


Figure 10. SEM micrographs and EDS results of ductile iron specimens containing a) 0 wt. % Al and 0 wt. % Cu, b) 4 wt. % Al, c) 4 wt. % Cu

3.3. Compressional properties

Compressive stress vs. strain curves of ductile iron containing 0 to 6 wt. % Al and 0 to 6 wt. % Cu are shown in Fig. 11. The figure illustrates that adding aluminum and copper to the ductile iron specimens

generally shifted the corresponding stress vs. strain curves upward, and the specimens endured greater stresses. The results obtained from stress vs. strain curves, including elasticity modulus, yield strength, maximum compressive stress, and fracture strain, are recorded in Table 2. The elasticity modulus, yield



strength, maximum compressive stress, and fracture strain of ductile iron specimen without any addition of aluminum and copper were 20.46 GPa, 134.2 MPa, 348.6 MPa, and 2.49%, respectively. Adding aluminum and copper to the ductile iron led to an increase in the modulus of elasticity. When 6 wt. % of copper and aluminum was added, elastic modulus increased to 47.63 GPa and 39.67 GPa, respectively. The yield strength, maximum compressive stress, and fracture strain were significantly improved by increasing aluminum and copper contents. It is noteworthy that the addition of aluminum had more influence on improving the mechanical properties of ductile iron specimens compared with copper. It is known that the addition of aluminum and copper elements leads to solid solution strengthening [37]. In addition, with the increase in the nodule count of graphite, the mechanical properties of ductile iron can be improved [38]. It is reported that the copper prevents crack growth in low levels of applied stress [39], and improves ultimate tensile strength, yield strength, and hardness [31]. In austempered ductile

irons, copper affects the amount of retained austenite, and consequently, enhances the impact energy [40].

4. Conclusions

In this study, ductile iron specimens containing 0, 2, 4, and 6 wt. % of aluminum and copper were manufactured by sand casting technique. The graphite morphology, microstructure, and mechanical properties were investigated, and the following conclusions were made.

The graphite morphology of the ductile iron was affected by the amount of aluminum and copper added to it.

Adding aluminum up to 2 wt. % resulted in a decrease in the surface fraction and nodule count of graphite, while for amounts greater than 2 wt. % they increased. By increasing aluminum, the nodularity of graphite increased.

Copper increased the surface fraction and nodule count of graphite and decreased the nodularity of graphite. With increasing copper, the amount of compacted graphite, compared with nodular graphite, increased.

Aluminum and copper affected the microstructure of ductile iron. With increasing aluminum and copper, the surface fraction of ferrite decreased and the surface fraction of pearlite increased.

Aluminum and copper had a significant influence on the mechanical behavior of ductile iron in compression. These additives could increase the modulus of elasticity, yield strength, maximum compressive stress, and fracture strain. The enhancing effect of aluminum additives on the compressive behavior of ductile iron was greater than copper additives.

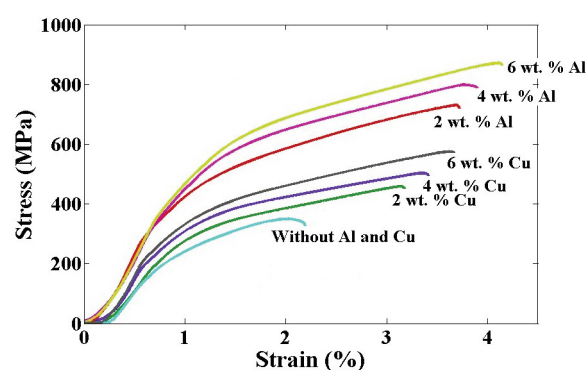


Figure 11. Compressive stress vs. strain curves of ductile iron specimens containing different amounts of aluminum and copper

Table 2. Compressional properties of ductile iron specimens containing different amounts of aluminum and copper

Alloying element	elastic Modulus /GPa	Yield strength /MPa	Maximum compressive stress/MPa	Fracture strain/%
Without Al and Cu	20.46	134.2	348.6	2.49
2 wt. % Al	41.31	179.4	752.6	3.71
4 wt. % Al	44.36	182.6	796.4	3.85
6 wt. % Al	47.63	188.8	874.5	4.21
2 wt. % Cu	28.04	142.6	452.2	3.27
4 wt. % Cu	36.78	149.8	488.4	3.41
6 wt. % Cu	39.67	151.4	572.8	3.67

References

- [1] J.A. Pero-Sanz Elorz, D.F. Gonzalez, L.F. Verdeja, Physical metallurgy of cast irons, Springer International Publishing, New York, 2018, p. 105.
- [2] D.M. Stefanescu, G. Alonso, P. Larranaga, E. Dela Fuente, R. Suarez, Acta. Mater., 107 (2016) 102-126.
- [3] D.M. Stefanescu, G. Alonso, P. Larranaga, E. De la Fuente, R. Suarez, Acta. Mater., 139 (2017) 109-121.
- [4] E. Guzik, Arch. Foundry., 21 (6) (2006) 33-41.
- [5] M. Kaczorowski, Arch. Foundry., 1 (2) (2001) 149-156.
- [6] A. Vadiraj, G. Balachandran, K. Kamaraj, J. Mater. Eng. Perform., 19 (7) (2010) 976-983.
- [7] M. Kaczorowski, A. Krzynska, Arch. Foundry., 18 (6) (2006) 84-92.
- [8] K.B. Rundman, J.R. Parolini, D.J. Moore, AFS. Transact., 145 (2005) 3-15.
- [9] S. Dymski, M. Trepczynski-Lent, Z. Lawrynowicz, Arch. Foundry., 6 (21) (2006) 21-29.
- [10] H. Pour Asiabi, 1st International Iron and Steel



- Symposium, April 2-4, Karabuk, Turkey, 2012, p. 126-131.
- [11] T. Sarkar, G. Sutradhar, Mater. Today. Proc., 4 (9) (2017) 10138-10143.
- [12] S. Panneerselvam, S.K. Putatunda, R. Gundlach, J. Boileau, Mater. Sci. Eng. A, 694 (2017) 72-80.
- [13] M.M. Jabbari Behnam, P. Davami, N. Varahram, Mater. Sci. Eng. A, 528 (2010) 583-588.
- [14] A. Janus, J. Kaczmar, Acta. Metal. Slovaca., 5 (2) (1999) 452-457.
- [15] W. Xue, Y. Li, J. Alloys Compd., 689 (2016) 408-415.
- [16] D. Medynski, A. Janus, Arch. Found. Eng., 3 (16) (2016) 59-66.
- [17] A. Janus, K. Granat, Arch. Civ. Mech. Eng., 4 (14) (2014) 602-607.
- [18] D. Medynski, A. Janus, Arch. Civ. Mech. Eng., 18 (2018) 515-521.
- [19] T. Sarkar, P.K. Bose, G. Sutradhar, Mater. Today. Proc., 5 (2018) 3664-3673.
- [20] N.V. Stepanova, I.A. Bataev, Y.B. Kang, D.V. Lazurenko, A.A. Bataev, A. Razumakov, A.M. Jorge Junior, Mater. Charact., 130 (2017) 260-269.
- [21] H.Y. Jung, M. Stoica, S. Yi, D.H. Kim, J. Eckert, Intermetallics., 69 (2016) 54-61.
- [22] H.Y. Jung, M. Stoica, S. Yi, D.H. Kim, J. Eckert, J. Mater. Res., 30 (2015) 818-824.
- [23] SK Shaha, MM Haque, AA Khan, Adv. Mater. Res., 264-265 (2011) 1928-1932.
- [24] E.E.T. EL-Sawy, M.R. EL-Hebeary, I.S.E. EL-Mahallawi, Wear., 390-391 (2017) 113-124.
- [25] X. Ding, X. Li, H. Huang, W. Matthias, S. Huang, Q. Feng, Mater. Sci. Eng. A, 718 (2018) 483-491.
- [26] Y. Liu, Y. Li, J. Xing, S. Wang, B. Zheng, D. Tao, W. Li, Mater. Charact., 144 (2018) 155-162.
- [27] A.D.A. Vicente, J.R.S. Moreno, T.F.D.A. Santos, D.C.R. Espinosa, J.A.S. Tenorio, J. Alloys. Compd., 775 (2019) 1230-1234.
- [28] S.M. Mostafavi Kashani, S.M.A. Boutorabi, J. Iron. Steel Res. Int., 16 (6) (2009) 23-28.
- [29] A. Zammit, S. Abela, L. Wagner, M. Mhaede, R. Wan, M. Grech, Surf. Coat. Technol., 308 (2016) 213-219.
- [30] P.W. Shelton, A.A. Bonner, J. Mater. Process. Technol., 173 (3) (2006) 269-274.
- [31] M. Gorny, E. Tyrala, G. Sikora, L. Rogal, Met. Mater. Int., 24 (1) (2018) 95-100.
- [32] N. Haghdadi, B. Bazaz, H. R. Erfanian-Naziftoosi, A. R. Kiani-Rashid, Int. J. Miner. Metall. Mater., 19 (9) (2012) 812-820.
- [33] H.R. Erfanian-Naziftoosi, N. Haghdadi, A.R. Kiani-Rashid, J. Mater. Eng. Perform., 21 (8) (2012) 1785-1792.
- [34] S. Liu, Y. Chen, X. Chen, H. Miao, J. Iron. Steel Res. Int., 19 (2) (2012) 36-42.
- [35] B. Y. Lin, E. T. Chen, T. S. Lei, J. Mater. Eng. Perform., 4 (5) (1995) 551-557.
- [36] A. M. Omran, G. T. Abdel-Jaber, M. M. Ali, Int. J. Eng. Res. Appl., 4 (6) (2014) 90-96.
- [37] M. Bahmani, R. Elliott, N. Varahram, J. Mater. Sci., 32 (1997) 4783-4791.
- [38] E. Akbarzadeh Chiniforush, N. Iranipour, S. Yazdani, China. Foundry., 13 (3) (2016) 217-222.
- [39] P.W. Shelton, A.A. Bonner, J. Mater. Process. Technol., 173 (2006) 269-274.
- [40] O. Eric, D. Rajnovic, S. Zec, L. Sidjanin, M.T. Jovanovic, Mater. Charact., 57 (2006) 211-217.

UTICAJ ALUMINIJUMA I BAKRA NA MORFOLOGIJU GRAFITA, MIKROSTRUKTURU I JAČINU MATERIJALA NA PRITISAK KOD NODULARNO LIVENOG GVOŽDA

H. Sazegaran ^{a,*}, F. Teimoori ^a, H. Rastegarian ^a, A.M. Naserian-Nik ^b

^a Tehnološki univerzitet Kučan, Katedra za industrijsko inženjerstvo, Tehnički fakultet, Kučan, Iran

^b Tehnološki univerzitet Kučan, Katedra za mašinsko inženjerstvo, Tehnički fakultet, Kučan, Iran

Apstrakt

U ovom radu je ispitan uticaj aluminijuma (0, 2, 4 i 6 wt. %) i bakra (0, 2, 4 i 6 wt. %) na morfologiju grafita, mikrostrukturu i jačinu materijala na pritisak kod uzoraka nodularno livenog gvožđa dobijenih tehnikom livenja u pesku. Morfologija grafita i mikrostruktura su ispitane pomoću optičke mikroskopije (OM) i softvera za obradu slika opremljenog skenirajućom elektronskom mikroskopijom (SEM). Za ispitivanje mehaničkih osobina izvedeno je ispitivanje materijala na pritisak na uzorcima nodularno livenog gvožđa. Rezultati su pokazali da su se prelomna površina i broj nodula grafita smanjili kada se količina aluminijuma povećala sa 0 na 2 wt.% i nakon toga sa 2 na 6 wt.%. Pored toga, nodularnost grafita se povećala sa povećanjem količine aluminijuma. Dodavanjem određene količine bakra povećale su se prelomna površina i broj nodula grafita, dok se nodularnost grafita smanjila. Dodavanjem aluminijuma i bakra smanjila se prelomna površina ferita, a povećala se prelomna površina perlita u mikrostrukturi. Povećanjem količina aluminijuma i bakra, krive jačine materijala na pritisak u odnosu na krive deformacije su pomerene na gore, a modul elastičnosti, opterećenje na istezanje, pritisni napon i jačina loma su poboljšani. U poređenju sa bakrom, aluminijum je imao veći uticaj na mehaničke osobine nodularno livenog gvožđa.

Cljučne reči: Nodularno liveno gvožđe; Bakar; Aluminijum; Morfologija grafita; Mikrostruktura; Jačina materijala na pritisak

